12. THERMAL CONTROL

To ensure the relative stability of the optical components within the Hipparcos payload, active and passive thermal control resulted in a temperature stability of better than 0.05 °C over short periods, and ±2 °C over the entire mission duration. Temperature measurements were collected at various points in the payload throughout the spacecraft's lifetime, and relayed both to the on-board computer (which monitors and regulates the thermal control) and the ground. Despite some loss of heater supply later in the mission, attributable to the excessive radiation damage experienced by the thermal control electronics, the payload thermal control proved to be extremely robust, permitting proper payload operation until the end of the mission.

12.1. Introduction

The thermal control of the Hipparcos payload was driven by very stringent requirements on the temperature stability of the payload structure, the optical elements and the detectors. Typical long-term temperature requirements were 20 ± 2 °C over the total mission duration when the payload was operational. Short-term temperature requirements on the mirrors were ±0.05 °C. These requirements could only be achieved by proper thermal design of enclosures, where the boundaries were used to balance internal and external thermal disturbances.

The payload structure was manufactured from carbon-fibre reinforced plastic with a very low coefficient of thermal expansion, using a box-type arrangement (see Figure 12.1). The optical elements and the detection systems were arranged inside the structure. In order to get isothermal boundaries, thin foil heater mats were placed on honeycomb panels (heater mat carriers), which were loosely connected mechanically to the carbon-fibre reinforced plastic structure. This design concept was chosen to minimise mechanical disturbance of the carbon-fibre structure due to thermal expansion of the honeycomb, and to keep the coefficient of thermal expansion constant by avoiding attaching a different material to the carbon-fibre structure. The entire payload was covered with multilayer insulation, except for two radiators, which were needed to dump the internally dissipated power of the detectors.

Depending upon the payload assembly, thermal control was achieved by either passive or active means, as shown in Table 12.1. The active thermal control relied on 21 'thermally

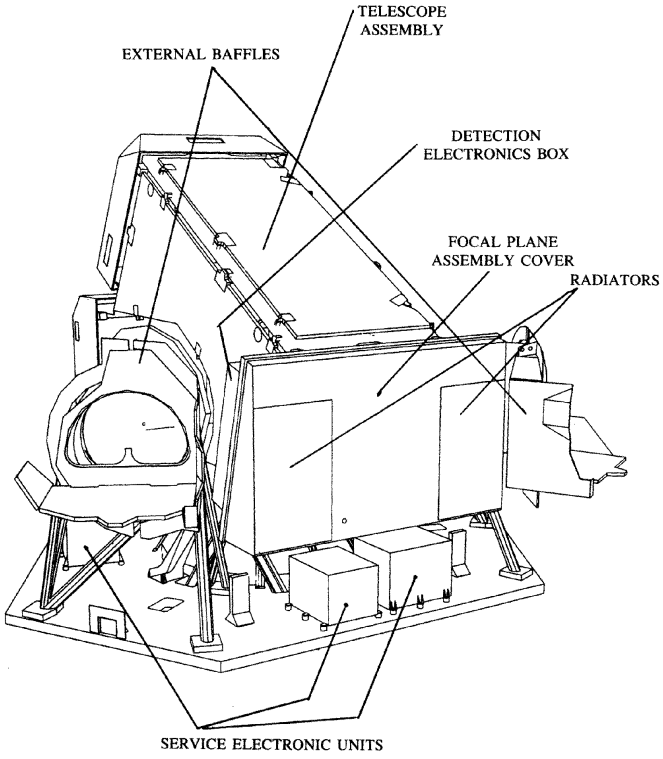

Figure 12.1. *Payload external configuration.*

controlled areas' (numbered from 1 to 24, with zones 4, 17 and 24 not used). Each area comprised a set of two heaters (nominal and redundant), physically implemented at the same location, and a set of two thermistors (nominal and redundant), implemented close to each other. These areas were controlled by the on-board computer through the thermal control electronics.

Active thermal control was provided to the payload, even when in the off state, by stand-by heaters controlled by the spacecraft electrical interface unit. There were two redundant automatic stand-by zones, corresponding to the telescope and the focal plane assembly. These zones were automatically regulated and the target temperatures were fixed; however, the heater's command could be over-ridden by ground command. There were two ground commanded stand-by zones (corresponding to the two detection electronics boxes).

For on-station payload operation, the heaters were controlled by a control law, monitored by the on-board computer, the principle of which is shown in Figure 12.2. Temperature measurements by the control thermistors were monitored by the thermal control electronics, and transmitted via the remote terminal unit to the on-board computer. The thermal control law, installed in the on-board computer, determined the respective power levels, which were sent back via the remote terminal unit and the thermal control electronics to the heater circuits. Updates were performed every 10 s. This system kept the mean temperature of the controlled area within 0.2 °C of the nominal values. Due to averaging, the individual optical elements within the enclosure were restricted to temperature excursions and temperature gradients of less than 0.05 °C.

Table 12.1. Characteristics of the payload thermal control.

Payload Assembly	Thermal Control	View to Space
Telescope assembly	active	yes
Focal plane assembly	active	no
Service electronics units	passive	no
Detection electronics boxes	active	no
Baffle assembly	passive	yes

12.2. Heater Design

The spacecraft thermal control provided a thermal environment to keep all of the spacecraft elements within their specified temperature limits throughout all the mission phases. In addition, it protected the payload from direct sun illumination in order to provide a more stable environment. The thermal control relied mainly on passive means, although for some critical elements supplementary heaters were provided. The thermal control electronics were in charge of controlling the tight payload thermal equilibrium. A certain number of areas had to be individually controlled in order to maintain the payload at the required temperature. Each of these areas contained a thermistor and a heater (see Figure 12.3 and Table 12.2).

The active thermal control worked mainly in the so-called proportional integral mode. Each heater was fed by a variable current level, which was driven in a closed-loop fashion by the reading of the relevant thermistor. For each cycle (10.66... s) the power fed to a heater was proportional to the difference between the actual temperature of the relevant controlled area and its target temperature. The overall control algorithm was located in the on-board computer, and based on so-called 'D-values' which for each heater identified a specific value of power (from 1–15) to be fed to the heater. Figure 12.4 presents the total power fed to the payload during the mission, expressed in units of D-values. In case of a degradation in the control area performance it was possible to inhibit the above described loop and put any control area in fixed power mode. This mode implied that the power applied to the heater was a constant value (on a scale of 1 to 15), defined on ground on the basis of the thermal history of the affected area.

12.3. Payload Thermal Control History

The first symptom of loss of heaters efficiency could be seen by the general increase of the on-board computer power level value fed to the heaters in order to keep each area at the target temperature. The second symptom was that once the maximum power level value had been reached or set manually (in fixed power mode) a decrease in the individual temperatures could be observed. The degradation could be observed by the need to increase the power load into the still functioning heaters to obtain a constant payload mean temperature (Figure 12.4, top), and the decrease of the payload mean temperature (Figure 12.4, bottom). During suspended operations, the mean payload temperature dropped to very low values since no on-board control on the thermal control electronics had been active.

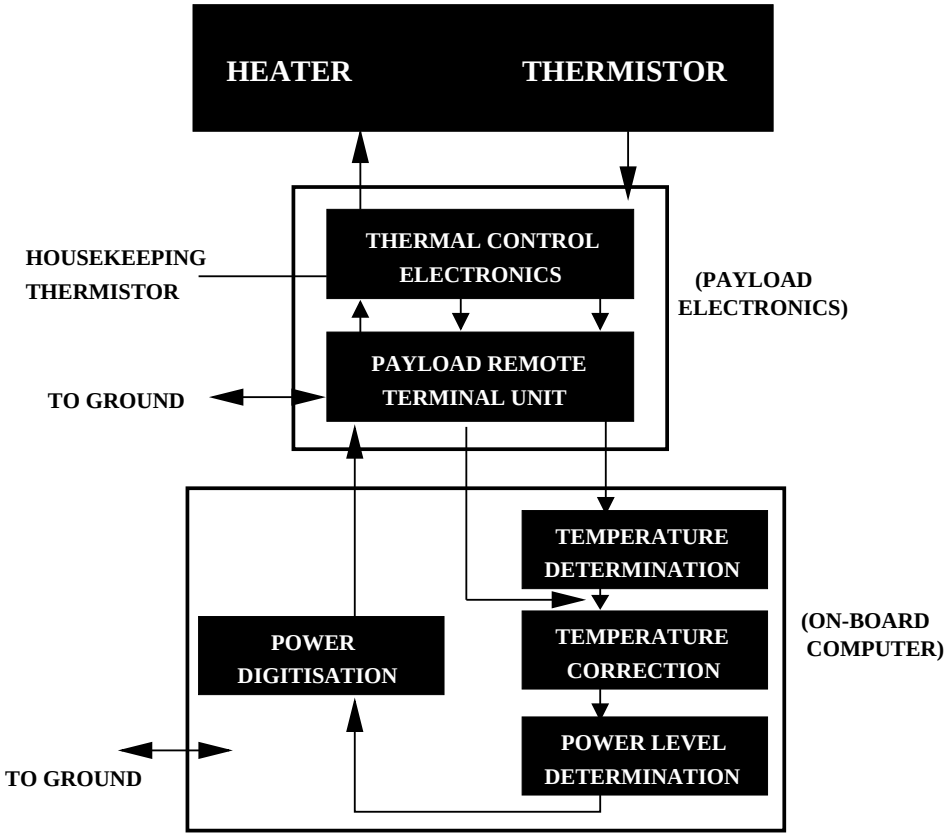

Figure 12.2. *Principles of the active thermal control.*

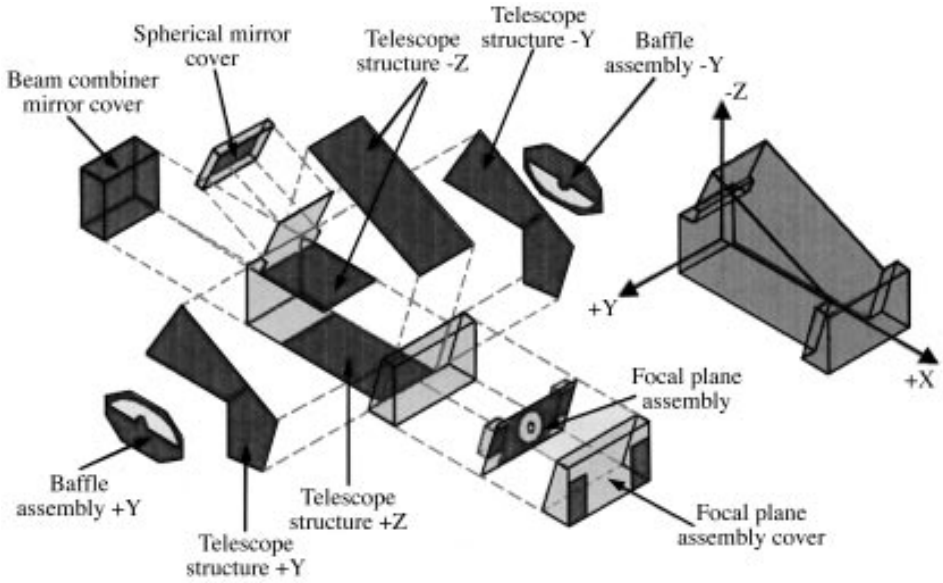

Figure 12.3. *Location of payload heaters.*

Table 12.2. Payload heater locations.

Payload Section	Heaters
Beam Combiner Mirror cover	heaters 1, 2, 3 and 5
Spherical Mirror cover	heater 7
Telescope Structure +Y	heaters 8 and 11
Baffle Assembly +Y	heater 15
Telescope Structure -Y	heaters 9 and 12
Baffle Assembly -Y	heater 16
Telescope Structure +Z	heaters 13 and 14
Telescope Structure -Z	heaters 6 and 10
Focal Plane Assembly	heaters 18, 21, 22 and 23
Focal Plane Assembly cover	heaters 19 and 20
Spares	heaters 4, 17 and 24

The following provides a summary of the changes occurring within the payload thermal control system during the mission (AR refer to formal 'Anomaly Reports', listed sequentially in Appendix B, and TCE refers to the Thermal Control Electronics):

90-07-19: AR number 37: loss of heater power supply on TCE 1 (area 17).

91-01-21: AR number 44: loss of heater power supply on TCE 1 (area 20).

91-01-25: Switch from TCE 1 to TCE 2.

91-09-18: TCE 2 area 20 set to fixed power mode value 11.

92-04-21: TCE 2 area 5 set to fixed power mode value 13.

92-07-06: AR number 61: TCE 2 loss of heater power supply (three heaters had now failed, three others were underperforming).

92-07-08: AR number 63: TCE 1 test (complete loss of the unit).

92-07-20: TCE 2 test (five heaters had now failed, two others were underperforming).

92-07-28: Payload TCE 1 and 2 tests (seven heaters had now failed).

92-09-02: Complete payload TCE 2 to fixed power mode.

93-02-10: TCE 1 and 2 test.

93-03-23: Payload off. TCE 2 left on.

93-03-24: TCE 2 configured to wide range to allow greater temperature variations.

93-03-30: All TCE 2 heaters to fixed power with value zero.

93-04-27: TCE 1 and 2 test. As further heaters had failed, all TCE 2 heaters were set to fixed power value 15.

93-06-07: TCE 2 test; out of 21 heaters only four were still functioning.

93-07-29: TCE 2 test.

During the mission lifetime a gradual degradation of the thermal control electronics 2 performance was noted since switch-on (on 25 January 1991), with occasional but significant peaks in the degradation rate (see Figure 12.4).

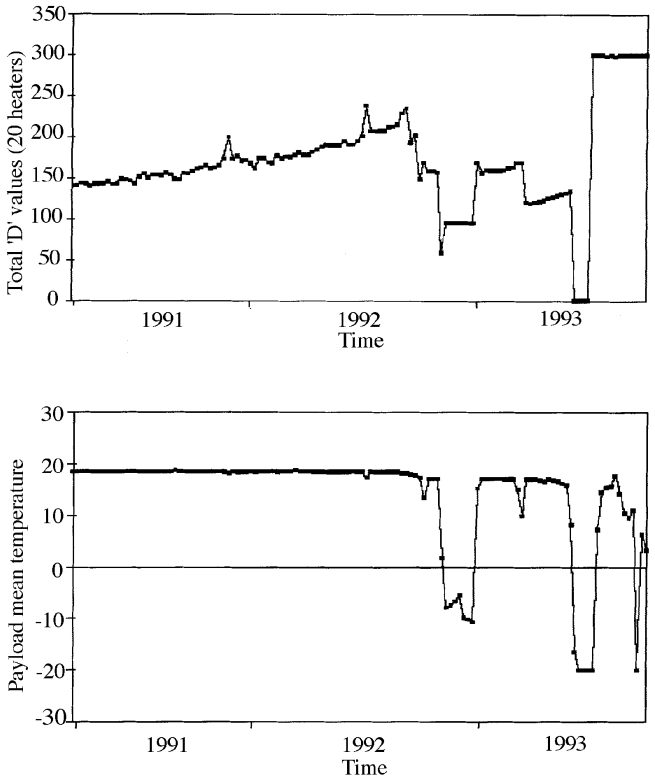

Figure 12.4. *Thermal control evolution throughout the mission. The top figure shows the total power fed to the payload, expressed in 'D values' (see text for details). The bottom figure shows the payload mean temperature (∘C) throughout the mission, including the low values experienced during suspended operations.*

12.4. Thermal Anomalies and the Basic Angle

The part of the payload most sensitive to temperature variations was the beam combiner. The basic angle, between the two viewing directions, had been specified to remain constant to within about 1 milliarcsec during a data set of up to 12 hours duration. It was therefore important to verify whether temperature control anomalies were the cause of rapid variations of the basic angle at the level of the great-circle reduction (see Figure 10.1, and also Volume 3, Chapter 9) observed on a few specific occasions during the mission.

Four thermistors controlled the surroundings of the beam combiner. Their temperature resolution was 0.03 K. It was found that temperature anomalies were indeed associated with significant variations of the basic angle. The characteristics of four such events during the first year of the mission are summarised in Table 12.3.

The basic angle results obtained in the FAST data reductions for the reference great circles around the above anomaly periods were investigated. In the basic data reduction treatment, the geometrical model (see Volume 3, Chapter 9) allowed only a constant value for the basic angle over the duration of one reference great circle. In most

Table 12.3. Payload temperature anomalies found during the interval studied.

year:day:hour	Temp. (K)	Anomaly Report (Appendix B)
1990:089:16	16.3	Payload remote terminal unit telemetry (AR26)
1990:118:11	20.5	On-board computer halted (AR29)
1990:243:14	17.9	Anomalous behaviour of on-board computer (AR38)
1990:322:04	19.0	

Table 12.4. Results for the reference great circle reductions solving for a variable basic angle. The model for the basic angle is $\gamma_0 + \gamma_1(t - t_0) + \gamma_2(t - t_0)^2$ where the times are expressed in days of 1990 (day 1.0 corresponding to 1 January 1990 0h UT). The angles are expressed in mas, mas/day and mas/day^2 (standard errors in parentheses).

t_0 (days)	$\gamma_0 - 58^\circ$ (mas)	γ_1 (mas/day)	γ_2 (mas/day^2)
89.715	31245.5 (0.3)	−3.8 (3.1)	18 (69)
90.121	31246.6 (0.3)	70.4 (1.7)	−452 (27)
90.560	31246.5 (0.4)	−7.0 (3.1)	60 (61)
118.575	31255.5 (0.3)	88.4 (4.1)	−1204 (132)
118.962	31248.3 (0.2)	−9.6 (1.4)	44 (18)
243.743	31249.0 (0.3)	86.8 (2.6)	−616 (40)
244.145	31243.9 (0.3)	−8.2 (1.8)	36 (21)
322.314	31244.7 (0.3)	80.6 (3.0)	−510 (54)
322.696	31242.4 (0.3)	−7.4 (1.3)	4 (15)

cases, during and after the anomaly, deviant values were found. Consequently, the great-circle reduction was repeated for all reference great circles associated with the temperature anomalies, and those immediately after. In these specific reductions, a quadratic variation with time was assumed for the basic angle. Although there was no reason to assume that such a model is particularly well suited to describe the basic angle variations, it had the advantage of being readily available in the software. A cubic model was not attempted because many of the data sets, in particular those during the most significant changes, were shorter than the minimum length required to apply such a model meaningfully. Table 12.4 gives the results obtained.

The basic angle indeed appeared to be responding to the temperature changes following a more-or-less fixed pattern: starting at a value of about 15 mas lower than the currently normal value, it increased quickly to a value above this normal value, and then returned to it much more slowly, on a time scale of about half a day. The rise sometimes seen at the end of the decreasing phase was never really significant, and was presumably an artefact of the quadratic model used to describe an exponential decrease.

In order to verify whether the low values at the start were real, or also due to the quadratic description, two of the reference great circles were reprocessed using only the first 4200 frames (i.e. one rotation plus one basic angle) allowing a constant basic angle and a linear variation with time. The results for these models were compared with those obtained previously, and confirmed the credibility of the initial low values of the basic angle.

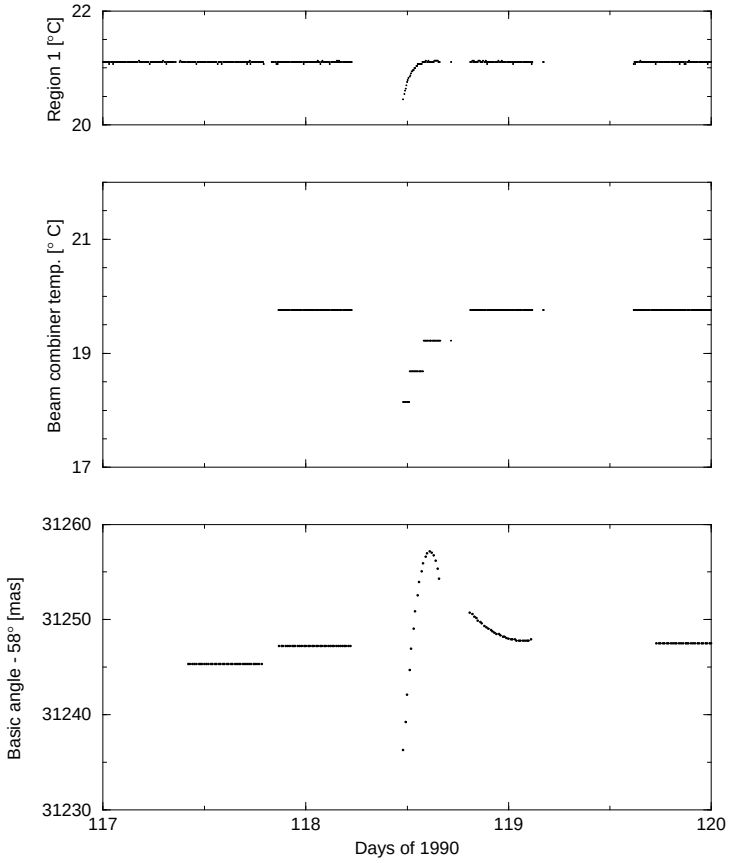

Figure 12.5. *Comparison of the temperature data of controlled region 1 (top), the beam-combiner housekeeping (thermistor) temperature reading (middle), and the basic angle variations arond the epoch 1990:118.*

Discussion

The behaviour of the basic angle during and after thermal control anomalies strongly suggests that two counteracting physical phenomena played a role, each with its own time scale. The first of these phenomena acted so as to decrease the basic angle, and responded (almost) immediately to changes in the temperature of the controlled regions, whereas the other phenomenon tended to increase the basic angle, and its effects were visible on a much longer time scale of about half a day.

It seems feasible that the more rapid effect was connected with the mounting of the beam combiner, and that the slower response was due to the interior of the beam combiner, possibly the glue cementing the two halves. In order to investigate this further, the output of the housekeeping thermistor on the beam combiner was checked. This thermistor was located on the back side of the beam combiner (near its edge) and is thus ‘halfway’ between the controlled regions and the interior. Although the resolution of the output was somewhat low (0.54 K), useful information could nevertheless be obtained.

Temperatures were derived from the telemetry values using the ESOC calibration curves. The temperatures from the thermistors were significantly lower than those of the controlled regions, which could be explained by the fact that the beam combiner radiated to the heat sinks presented by the baffles and open space.

In order to permit a better comparison, the controlled region temperatures, housekeeping thermistor temperature, and basic angle evolution for the two more obvious cases were combined. From this, it was clearly evident that the beam combiner temperature reacted much more slowly after a temperature anomaly (on a timescale of order 10 hours) than the controlled region temperature (on a timescale of 2–3 hours). This seemed to confirm the above hypothesis of a fast and a slower effect combined (see Figure 12.5).

An extra tilt of the beam combiner could explain the decrease in basic angle, but it would also have caused a very significant increase in differential field rotation. No evidence for this was found in the geometrical calibration, so that this explanation does not appear to be valid.